Computing quark polarized momentum fraction in the Nucleon from lattice QCD at the physical pion mass

Constantia Alexandrou[1,2], Simone Bacchio[2], **Priyajit Jana**[1,2], Giannis Koutsou[2], Yan Li[2], and Gregoris Spanoudes[1]

[1]Department of Physics, University of Cyprus, Nicosia, Cyprus
[2]Computation-based Science and Technology Research Center, The Cyprus Institute

1. The Nucleon Spin Puzzle

Nucleons (Nucleons and neutrons) make up most of the visible mass in the Universe, and each one *spins* with angular momentum $\frac{1}{2}$. Nucleons are made of quarks and gluons. Early experiments showed that the quark helicity accounts for only a fraction of the Nucleon's spin [1], motivating the study of nucleon spin structure.

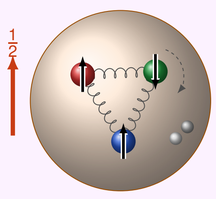

2. Probing Spin in Experiments

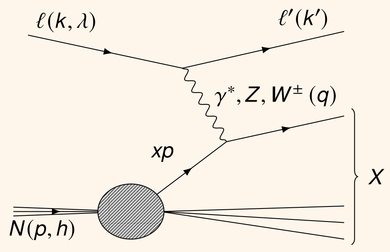

Figure: Deep-inelastic scattering (DIS) at leading order (adapted from [2]).

- By comparing scattering rates for *aligned* and *anti-aligned* beam and nucleon spins, experiments determine how quark helicities are distributed inside the Nucleon. Measurements at CERN COMPASS experiment, Jefferson Lab, and RHIC have progressively constrained these distributions.
- Global analyses by BDSSV, NNPDF, JAM and MAP [12, 13, 14, 15] combine all data to extract $\Delta q(x)$.
- However, the **small-x region remains poorly constrained**, making the full x-dependence difficult to determine experimentally. The **Electron–Ion Collider** [3] will extend the reach to much smaller x.
- **Lattice QCD** provides an independent, first-principles calculation of *moments* of these distributions, without reconstructing their full x-dependence.

3. From 3D Structure to Moments

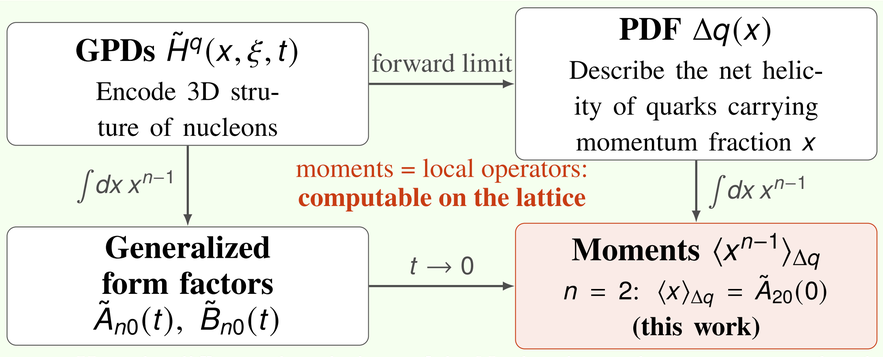

Figure: How the different descriptions of the Nucleon's quark structure are related.

- **GPDs** are a powerful tool to probe the 3D structure of nucleons and bridge the gap between spatial and momentum distributions of quarks gluons within nculeons, measured in exlcusive processes such as deeply virtual Compton scattering.
- In the zero moemtum limit they reduce to the **PDF** $\Delta q(x)$: the distribution of polarized momentum fraction x carried by quarks of flavor q.
- PDFs and GPDs cannot be computed directly on a Euclidean lattice, but their **x-moments** can: they are matrix elements of *local* operators, calculable from first principles, with systematic effects controlled by simulating at several lattice spacings and physical quark masses.
- $n = 1$: $\int dx\, \Delta q(x)$ is the net quark helicity. $n = 2$ **(this work)**: the quark helicity weighted by the momentum fraction x, which is also related to quark spin–orbit correlations [7]:

$$\langle x \rangle_{\Delta q} = \int_0^1 dx\, x \left[\Delta q(x) - \Delta \bar{q}(x) \right]$$

4. Lattice QCD

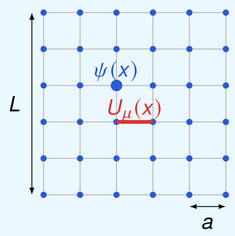

quarks ψ on sites,
gluons U_μ on links

- **Why it is needed:** quantum chromodynamics (QCD) describes the strong interaction between quarks and gluons. At low energies the coupling is strong and the perturbative expansion fails, so a non-perturbative approach is needed to describe hadrons.
- **The idea** [8]: formulate QCD on a discrete 4D Euclidean space-time lattice (spacing a, size L) with exact gauge symmetry. The path integral becomes finite-dimensional and is evaluated by Monte Carlo importance sampling.
- **First-principles approach:** the only inputs are the quark masses and the strong coupling. Continuum results ($a \to 0$) are obtained by extrapolating from several lattice spacings.

Ensemble [9]	a [fm]	L [fm]	M_π [MeV]
cB211.072.64	0.0796	5.09	140
cC211.060.80	0.0682	5.46	137
cD211.054.96	0.0569	5.46	141
cE211.044.112	0.0489	5.48	137

Four lattice spacings
at the **physical pion mass**
$\Longrightarrow$ continuum limit $a \to 0$

$N_f = 2 + 1 + 1$ twisted-mass clover fermions (ETMC)

5. Extracting the Nucleon Matrix Element

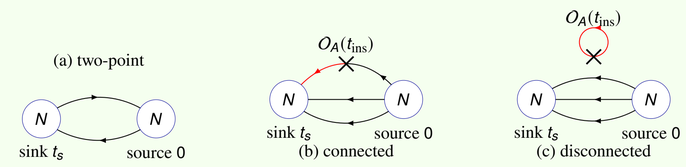

Figure: Diagrams of (a) the nucleon two-point function and (b, c) the three-point function of two different type of contributions.

(i) Two-point function. An interpolating field creates a state with the nucleon's quantum numbers at the source and annihilates it at the sink, a Euclidean time t_s later (a). Excited states decay faster, so at large t_s only the ground state survives:

$$C_{2\text{pt}}(t_s) = \sum_n |Z_n|^2 e^{-E_n t_s} \xrightarrow{t_s \text{ large}} |Z_0|^2 e^{-E_0 t_s}.$$

(ii) Three-point function. The operator $O_A^{\mu\nu} = \bar{q}\, \gamma^{\{\mu} \gamma_5 \overleftrightarrow{D}^{\nu\}} q$ is inserted at an intermediate time t_{ins}. Evaluating the quark contractions yields two different diagrams: a *connected* diagram (b) where the operator probes a valence quark propagating from source to sink, and a *disconnected* diagram (c) where it probes a closed sea-quark loop interacting with the nucleon via gluons.

(iii) Ratio. The overlaps Z_0 and time dependence cancel, leaving the matrix element (up to kinematic factors):

$$\frac{C_{3\text{pt}}(t_s, t_{\text{ins}})}{C_{2\text{pt}}(t_s)} \xrightarrow{t_{\text{ins}},\ t_s - t_{\text{ins}} \text{ large}} \langle N |\, O_A^{\mu\nu}\, | N \rangle.$$

Remaining excited-state effects are removed with two-state (connected) and plateau (disconnected) fits.

(iv) Decomposition. In the forward limit, Lorentz symmetry ensures this matrix element is proportional to a single physical quantity—our desired moment:

$$\langle N(p,s) |\, O_A^{\mu\nu}\, | N(p,s) \rangle \propto \tilde{A}_{20}^q(0) \quad \Longrightarrow \quad \boxed{\langle x \rangle_{\Delta q} = \tilde{A}_{20}^q(0)}.$$

The bare result is renormalized non-perturbatively (RI′-MOM) and converted to $\overline{\text{MS}}$ at $\mu = 2$ GeV.

6. Results

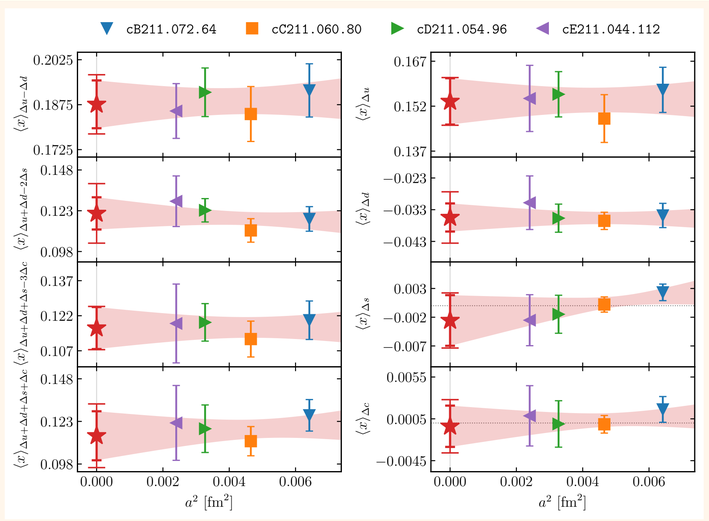

Figure: Continuum limit: results on the four different lattice spacings extrapolated to continuum $a^2 \to 0$ (band), using constant and linear fits combined by model averaging.

Key results ($\overline{\text{MS}}$, 2 GeV, continuum)

$$\langle x \rangle_{\Delta u - \Delta d} = 0.1876(80)(56)$$
$$\langle x \rangle_{\Delta u} = 0.1536(77)(25)$$
$$\langle x \rangle_{\Delta d} = -0.0350(23)(16)$$
$$\langle x \rangle_{\Delta s} = -0.0026(44)(19)$$
$$\langle x \rangle_{\Delta c} = -0.0004(26)(20)$$

Up quarks are preferentially **aligned** with the Nucleon spin, **down quarks** preferentially **anti-aligned**. Strange and charm contributions are small.

Flavor results from singlet/non-singlet combinations and from direct per-flavor extrapolation are consistent.

7. Comparison with Phenomenology and Other Lattice Studies

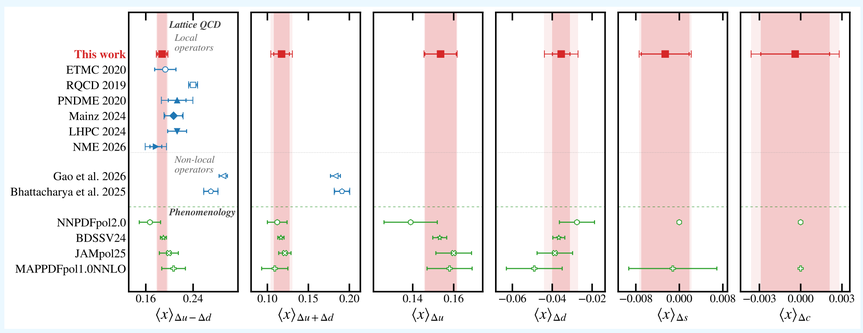

- Our results are **consistent** with recent global analyses of experimental data [12, 13, 14, 15] and with lattice calculations based on local operators.
- Recent calculations using non-local operators give somewhat larger central values; the differences may reflect different lattice setups and analysis methods.

Conclusions

- Moments of parton distributions connect experimental measurements with first-principles lattice QCD.
- We compute the second moments of the nucleon polarized PDF using only physical point ensembles, thus eliminating the need for chiral extrapolation.
- **Next:** gluon contribution, higher moments and the reconstruction of the full x-dependence.

References

[1] J. Ashman *et al.* [EMC], Phys. Lett. B **206** (1988) 364.
[2] I. Borsa, D. de Florian, I. Pedron, arXiv:2210.12014 [hep-ph].
[3] A. Accardi *et al.*, Eur. Phys. J. A **52** (2016) 268.
[4] X. Ji, Phys. Rev. Lett. **78** (1997) 610.
[5] M. Burkardt, Phys. Rev. D **62** (2000) 071503.
[6] M. Diehl, Phys. Rept. **388** (2003) 41.
[7] C. Lorcé, Phys. Lett. B **735** (2014) 344.
[8] K. G. Wilson, Phys. Rev. D **10** (1974) 2445.
[9] C. Alexandrou *et al.*, Phys. Rev. D **101** (2020) 034519.
[10] S. Mondal *et al.*, arXiv:2608.02836 [hep-lat].
[11] I. Borsa *et al.*, Phys. Rev. Lett. **133** (2024) 151901.
[12] J. Cruz-Martinez *et al.*, JHEP **07** (2025) 168.
[13] C. Cocuzza *et al.*, Phys. Rev. D **112** (2025) [arXiv:2506.13616].
[14] V. Bertone *et al.*, Phys. Lett. B **865** (2025) 139497.

Acknowledgements

This work is supported by the projects DeNuTra, PulseQCD, and MuonHVP, co-funded by the European Union under the Cohesion Policy Programme "THALIA 2021–2027". This work also acknowledges partial support from the projects IMAGE-N (EXCELLENCE/0524/0459), StrongILA (EXCELLENCE/0524/0001), and partonWF (VISION ERC/0525/0010) funded by the European Regional Development Fund and the Republic of Cyprus through the Cyprus Research and Innovation Foundation.

Republic of Cyprus

Co-funded by the European Union